Mon. Not. R. astr. Soc. (1990) **246**, 616–623

Chemical evolution of spiral galaxies: models with star formation proportional to molecular hydrogen

M. Tosi
Osservatorio Astronomico, CP 596, I-40100 Bologna, Italy

A. I. Díaz
Departamento de Física Teórica, Universidad Autónoma de Madrid, Spain

Accepted 1990 May 1. Received 1990 April 30; in original form 1990 March 14

SUMMARY

The possibility of assuming the star formation-rate ψ in spiral discs to be proportional to their H_2 density is analysed. Since a good correlation between the molecular gas fraction and the logarithm of the oxygen abundance is derived from a sample of several nearby spirals, we examine in particular the possibility that $\psi \propto \Sigma H_2/\Sigma_{gas} \propto \log(O/H)$.

Numerical models have been computed to evaluate the implications on the chemical evolution of spiral galaxies of two alternative assumptions on this kind of star-formation rate. In one case ψ is always proportional only to H_2 through the empirical relation found with the oxygen abundance, and in the other it is proportional to both the H_2 and the total gas density. Model results are presented for the Galaxy and for the spirals M31, M83, M101 and NGC 2403. It is found that some of these models' predictions are in less good agreement with the data than those based on star-particular, the assumption of bimodal dependence of the star formation on the two gas components applies rather well to the galaxies in our sample. However, these models' predictions are in less good agreement with the data than those based on star-formation rates exponentially decreasing with time.

1 INTRODUCTION

The knowledge of the correct law of star formation is of primary importance to the understanding of galaxy evolution, but unfortunately the actual processes of stellar formation are still poorly known. People studying the chemical evolution of galaxies have tried to overcome this difficulty by parametrizing the star-formation rate (SFR) in various ways. All these parametrizations have reasonable physical bases, but none of them is really satisfactory (e.g. Tosi 1990 and references therein). One of the most appealing suggestions (e.g. Rana & Wilkinson 1986, hereafter RW86) of the last few years is that the SFR be related to the H_2 density (ΣH_2) rather than to the neutral-hydrogen (ΣH I) or total-gas density [$\Sigma_{gas} = 1.41(\Sigma H\,I + \Sigma H_2)$ to take helium into account]. In fact, the radially declining SFRs inferred from observations in the discs of nearby spirals do not resemble the flat distributions of H I or total gas and are more consistent with (though not equal to) that of H_2. Besides, young stars (i.e. star-forming regions) in the Galaxy and in nearby spirals are indeed associated with molecular clouds.

A major difficulty in checking the actual relation between ΣH_2 and the star-formation rate resides in the lack of direct H_2 measurements. As is well-known, the H_2 content is inferred from submillimetric observations of CO, under the assumption that the two quantities are tightly correlated (e.g. Young & Scoville 1982; Sanders *et al.* 1984). The conversion factor between CO and H_2, however, is uncertain at least by a factor of 3 (e.g. Bhat *et al.* 1984), and the possible differential effect of metallicity variations on CO and on H_2 adds another significant uncertainty. For instance, the fact that regions of very active star formation but low average metallicity, such as blue compact galaxies, show no evidence of CO (which might be explained in terms of the above differential effect) gives an idea of the difficulty in studying the correlation between SFR and H_2 content. Besides, there are neither direct nor indirect means to evaluate the past H_2 content even in the most local neighbourhood, and this prevents any hypothesis on the past SFR.

In order to find a way to overcome these difficulties and to correlate the SFR with H_2, other relations between H_2 and measured quantities have been looked for. For instance,

since the formation of H_2 depends on the availability of grains in the interstellar medium, RW86 have suggested that the molecular gas fraction $\Sigma H_2/\Sigma_{gas}$ is proportional to some power b of the ambient metallicity Z, which can be reliably derived for objects in a large range of distances and ages.

Starting from their suggestion, we have re-analyzed the empirical relations between molecular gas fraction and metallicity, found a different relation from that proposed by Rana & Wilkinson (1988, hereafter RW88), and examined in some detail the corresponding implications for the chemical evolution of spiral galaxies. To this end, we have computed several numerical models for the evolution of the Galaxy and four nearby spirals based on different assumptions on the SFR–metallicity relation. The results of these models are described and discussed.

2 EMPIRICAL RELATIONS BETWEEN MOLECULAR HYDROGEN AND METALLICITY

From the data on gas densities and H II region abundances collected from the literature by Díaz & Tosi (1984) and Tosi & Díaz (1985, hereafter TD85) for several nearby spirals and the Milky Way, RW88 have inferred that the relation $\Sigma H_2/(\Sigma H\,I+\Sigma H_2)\propto Z^{1.3}$ derived by RW86 for the Milky Way holds for the entire sample of spirals. Given the uncertainty on the CO–H_2 conversion factor inherent in the determination of the gas density, they checked the above relation for both the factors given by Sanders *et al.* (1984) and by Bhat *et al.* (1984) and found that the latter is preferable, at least for the Galaxy (RW86). They then argue that a star-formation rate $\psi\propto\Sigma H_2^k\propto(\Sigma_{gas}XZ_{16}^{1.3})^k$, where X and Z_{16} are the abundances by mass of hydrogen and oxygen, may be valid for all these spirals.

From the same data, however, we find that a better agreement to the whole set of galaxies is found if the linear value of $\Sigma H_2/\Sigma_{gas}$ is plotted instead of the logarithmic value. The least-squares fit to the data gives

$$\Sigma H_2/\Sigma_{gas}=0.37[12+\log(O/H)]-2.99. \quad (1)$$

Our relation is represented by the solid line in Fig. 1, where the data relative to different galaxies are indicated by different symbols. By comparing this figure with fig. 1 of RW88, the different quality of the two fits can be deduced, especially for the metal-rich–H_2-rich part of the diagram.

It is apparent from our figure that, within some of the spirals (e.g. the almost vertical distribution of the diamonds representing the data of M31), there are large deviations from the best-fitting relations, but the overall dispersion is fairly small. It is important to note, however, that the relation must presumably deviate from the linear regime at the low-metallicity end of the considered range to avoid the unrealistic consequence of a negative ΣH_2 content. This implies that our relation cannot be extrapolated outside the observational range $8\leq 12+\log(O/H)\leq 10$. The lack of CO detections in low-metallicity galaxies is an additional indication of our ignorance about the lower left part of the diagram of Fig. 1. This caveat should be kept in mind before applying this same relation to galaxies of lower overall metal content.

Both the above relations have been derived from the data on H II regions and molecular clouds, and therefore refer only to the young components of galactic discs. Since we have no information on the past H_2 distribution, for the sake of the argument and to check the suggestion of RW88, in the following we will make the strong and arbitrary assumption that these relations also apply to older objects, and use them to derive the past H_2 content of the examined galaxies. Since the metal abundances of galaxies of any morphological type have probably increased with time, the above relations imply that $\Sigma H_2/\Sigma_{gas}$ is also an increasing function of time.

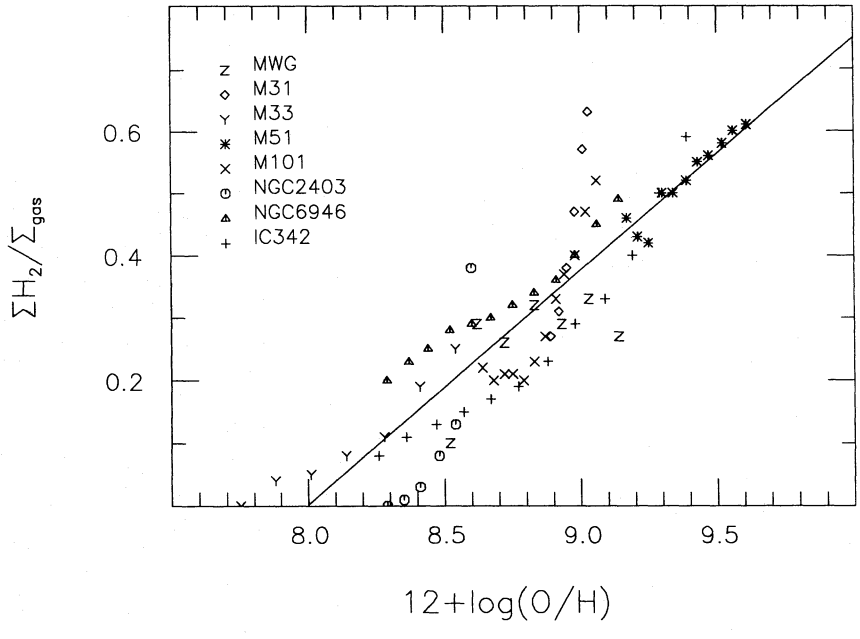

Figure 1. Relation between the molecular gas fraction and the oxygen abundance for the spirals M31, M33, M51, M101, NGC 2403, NGC 6946 and IC342.

3 CHEMICAL-EVOLUTION MODELS

We have computed several models of galactic chemical evolution to investigate if SFRs which are proportional to the molecular gas fraction and follow the empirical relations described in the previous section, predict results consistent with the observational data available for the Galaxy and other well-studied spirals. We have examined three types of models, which by no means cover all the possible hypotheses on the SFR dependence on H_2, but can give a general idea of its implications. The models are of the kind described by TD85 and Tosi (1988, hereafter T88). We assume Tinsley's (1980) initial mass function (IMF), constant in space and time and extrapolated to 100 $M_\odot$, standard stellar-evolution models, and no instantaneous recycling approximations.

3.1 ΣH_2 proportional to $Z_{16}^{1.3}$

Following RW88 we have first assumed

$$\psi_{RW} \propto \Sigma H_2^k = A(\Sigma_{gas} X Z_{16}^b)^k, \qquad (2)$$

where b is an exponent which they assume equal to 1.3, k is the usual exponent of the Schmidt law, and A is a coefficient, constant in time but slightly varying with galactocentric distance. For the initial phases of the disc evolution we have adopted $X \simeq 0.77$ and $Z_{16} = 10^{-5}$, which roughly correspond to Population II abundances. Since the initial metallicity is low, if the proportionality constant A is small, the star formation is totally inefficient and does not allow any evolution. But if A is large enough to let the evolution start, then the rapid increase of Z triggers such a large increase in ψ that the disc gas is consumed almost immediately and the metal abundances reach values larger than those ever observed in spirals.

3.2 ΣH_2 proportional to 12 + log(O/H)

If we assume the SFR to be proportional to ΣH_2, then the empirical relation between the molecular gas fraction and the oxygen abundance by number given by equation (1) implies

$$\psi_2 \propto \Sigma H_2^k = B\{0.37\Sigma_{gas}[12 + \log(O/H)] - 2.99\Sigma_{gas}\}^k. \qquad (3)$$

As mentioned in Section 2, however, this relation can be applied only in the observational range $8 \leq 12 + \log(O/H) \leq 10$, where equation (1) is derived. We then do not know what SFR should be adopted for the initial epochs, when $12 + \log(O/H) < 8$ and a linear extrapolation of equation (3) would provide the unphysical result of a negative SFR. We suggest here two possible ways out of the problem.

(i) The extrapolation of equation (1) at the low-abundance end is given by the RW88 exponential relation, and the SFR is therefore provided by equation (2) for $12 + \log(O/H) < 8$, and by equation (3) for $12 + \log(O/H) \geq 8$.

(ii) The good correlation between ΣH_2 and $12 + \log(O/H)$ does not imply that the SFR be proportional *only* to the metallicity, and we therefore assume a bimodal SFR resulting from the combination of equation (3) with a Schmidt law. In this case, $\psi_b = \psi_1 + \psi_2$, where $\psi_1 = C\Sigma_{gas}^k$ and is always active until the gas is exhausted, and ψ_2 is defined as in equation (3) and works only for $12 + \log(O/H) \geq 8$.

The flat extrapolation of case (i) and the dependence of ψ_b on the total-gas density of case (ii) both guarantee the continuity and the smoothness of the SFR of these models. Due to their different expressions, however, the time behaviour of the SFR is quite different in the two cases. In case (i) there is a strong initial activity, corresponding to the exponential relation of equation (2), which rapidly (i.e. within about 10^7 yr) produces the amount of oxygen required to switch to the linear mode. At that point there is a significant reduction of the SFR, followed by a slow increase up to the present epoch. In case (ii) the Schmidt-law component is always active and tends to reduce the SFR monotonically with time, due to the corresponding gas consumption. However, if B is at least equal to C, when log(O/H) is large enough ψ_b becomes more sensitive to the metallicity, and increases steadily. The combination of the two competing modes generally results in a very slow time decrease of the SFR and allows the reproduction of several observed properties of spiral galaxies which cannot be obtained by simple Schmidt laws.

The parameters allowed to vary in these models are the exponent k, the proportionality constants B and C and the infall rate. To find the best values of these parameters, we have compared the model results with the corresponding observational constraints available for the Milky Way and nearby spirals.

4 RESULTS AND DISCUSSION

We have already seen that the chemical-evolution models based on the RW88 relation and examined in Section 3.1 do not provide realistic results. To check the validity of the models proposed in Section 3.2, we have first compared their predictions with the observational data of our own Galaxy, which are more numerous and reliable. We have modelled also the evolution of the other spirals, adopting the same

Table 1. Parameters and results of the models of case (i).

model	k	B/C	infall	χ^2_{SFR}	$\chi^2_{O/H}$
1	1.0	1.0	-	2.5	7.8
2	1.0	2.0	-	1.3	1.3
3	1.0	2.5	-	1.1	0.8
4	1.0	3.0	-	1.4	1.5
5	1.0	6.0	-	2.3	3.3
6	1.2	2.0	-	3.6	6.8
7	1.2	4.0	-	2.3	1.6
8	1.2	5.0	-	2.1	0.9
9	1.2	6.7	-	1.4	0.6
10	1.2	10.0	-	0.8	2.3
11	1.2	15.0	-	1.0	1.9
12	1.2	30.0	-	2.3	1.3
13	1.3	2.0	-	4.2	10.3
14	1.3	10.0	-	2.1	0.6
15	1.3	25.0	-	6.0	2.0
16	1.4	10.0	-	4.2	1.5
17	1.4	20.0	-	1.8	1.3
18	1.4	30.0	-	3.6	1.3
19	2.0	2.0	-	1.9	19.9
20	2.0	3.0	-	2.8	0.5
21	2.0	10.0	-	3.5	0.6
22	2.0	40.0	-	7.6	1.5
23	1.0	2.0	0.001	1.4	1.5
24	1.0	1.0	0.003	3.9	1.0
25	1.0	2.0	0.003	2.6	0.6
26	1.0	4.0	0.003	3.3	0.7
27	1.0	10.0	0.003	2.0	4.9
28	1.0	2.0	0.05M	1.5	1.4
29	1.0	2.0	0.10M	1.8	1.1
30	1.2	10.0	0.05M	1.0	1.8
31	1.2	10.0	0.10M	1.8	1.5
32	1.3	10.0	0.05M	2.5	0.6
33	1.3	10.0	0.10M	3.0	0.7

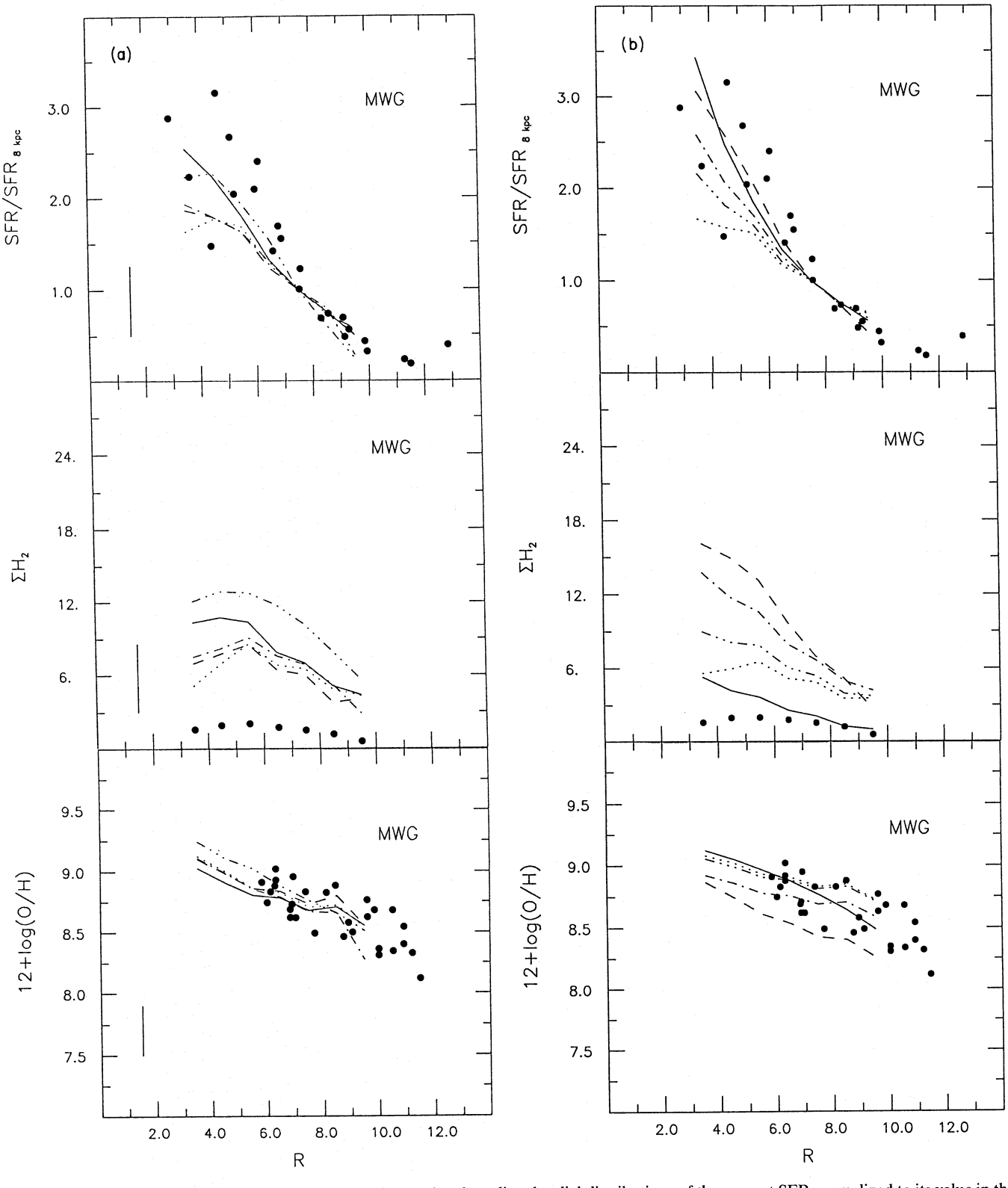

Figure 2. Milky Way galaxy: comparison between observed and predicted radial distributions of the current SFR normalized to its value in the solar neighbourhood (top), H_2 density in $M_\odot$ pc^{-2} (centre), and oxygen abundance by number (bottom). The dots correspond to the observational data and the average error bar for each set of data is shown. Fig. 2(a) (left) corresponds to the case (i) models 2 (solid line), 17 (dash-three-dotted), 22 (dashed), 33 (dash-dotted) and 43 (dotted) of Table 1. Fig. 2(b) (right) shows a *standard* model (solid line) and the bimodal models 2 (dash-three-dotted), 3 (dash-dotted), 10 (dashed) and 28 (dotted) of Table 2.

parameter values which give the best agreement with the Galaxy constraints.

4.1 The Galaxy

For the Galaxy, Table 1 lists the case (i) models which provide sensible results. The values of the $\chi^2=\Sigma_i(O_i-P_i)^2/\sigma_i^2$ derived from the comparison of the observed O_i and predicted P_i present values in all galactic rings, i, of the SFR, and of the oxygen abundances are given for each model. These values take into account the observational error, σ, and are normalized to the number of observed data. They are thus acceptable only if they are around 1. The data on the SFR are taken from Lacey & Fall's (1985) collection of 19 measurements derived from observations of pulsars, supernovae and Lyc photons within the range of galactocentric distances covered by our models. They are shown in the top panel of Fig. 2(a). The data on the H_2 density are presented in the central panel of Fig. 2(a) and are derived from Talbot (1980). The data on the oxygen abundances are taken from Shaver *et al.*'s (1983) radio and optical observations of 29 H II regions, and are shown in the bottom panel of Fig. 2(a). In each panel the average error bar is drawn. Also shown are some of the case (i) models more consistent with the empirical data (models 2, 17, 22, 33 and 43 of Table 1). The agreement is quite good, except for the ΣH_2 distribution.

Column 4 of Table 1 gives the infall-rate density in $M_\odot$ kpc^{-2} yr^{-1}, assumed to be uniform all over the disc (*equidense* models in T88) except in the last block, where the infall rate is assumed proportional to the total mass, M, of the region and therefore decreasing outwards (*parametric* models in T88). The e-folding time of the infall rate is taken equal to ∞ in all cases, except in the models of the third block of Table 1, where it is 5 Gyr. It is apparent from Table 1 that the assumption of constant and uniform infall-rate density tends to worsen the agreement with the observations, unless the infall rate is small enough (e.g. the dashed line in Fig. 2a, corresponding to model 22 where the infall-rate density is 1×10^{-3} $M_\odot$ kpc^{-2} yr^{-1}). A few models assuming an infall-rate density decreasing with galactic radius (last block of Table 1) are also in reasonable agreement with the observed data (dotted line of Fig. 2a representing model 43).

Columns 2 and 3 of Table 1 list, respectively, the exponent k and the proportionality constant B of the SFR. The latter is in units of 10^{-2} (pc^2 yr^{-1})^k. A general result of these models is that the lower the exponent k, the better the agreement with the observational constraints (e.g. the central panel of Fig. 2a). Naturally, since both a larger k and a larger B enhance the star formation, to get sensible results the exponent and the constant of the SFR turn out to be inversely proportional. In fact, Table 1 shows that in the best models B is around 3 for $k=1$, whilst it is in the range 0.05–0.06 for $k=2$.

Table 2 provides the same information as Table 1, but for the case (ii) models. Column 3 lists the ratio between the proportionality constant of the molecular-gas mode and that of the total-gas mode. Column 4 of Table 2 gives the infall-rate density in $M_\odot$ kpc^{-2} yr^{-1} assumed to be uniform over all the disc except in the last block where the infall-rate is assumed proportional to the total mass M of the region.

These models listed in Table 2 that are more consistent with the observational constraints of the Galaxy are shown in Fig. 2(b) (models 2, 3, 10 and 28). The solid line in each of the three panels of Fig. 2(b) refers to a *standard* model with $\psi\propto e^{-t/\tau}$ ($\tau=15$ Gyr) and constant and uniform infall, $F=4\times10^{-3}$ $M_\odot$ kpc^{-2} yr^{-1}, found by TD85 and T88 to be one of the best models for our Galaxy. It is interesting to note that this *standard* model is indeed more consistent with the data of Fig. 2 than any of the models computed here. This is particularly evident for the H_2 present distribution: an unfortunate result for an SFR like ours based just on this distribution!

Once again we find that the exponent k should be smaller than 2, to avoid inconsistent predictions on the various quantities (like a present SFR increasing outwards), and its best value ranges between 1 and 1.2. We find that the constant B should be larger than C by a factor of 2–10, and in the range 10^{-3}–10^{-2} (pc^2 yr^{-1})^k. Finally, note that most of the bimodal models in better agreement with the observations, assume no infall of gas from outside the disc, contrary to what is generally found with more standard models (e.g. Tosi 1990 and references therein). Even more striking is the fact that the only models which have infall and are consistent with the data assume an infall-rate density which decreases with galactocentric distance. This is because an equidense infall brings proportionally more gas to the outer galactic rings.

Table 2. Parameters and results of the bimodal models of case (ii).

model	k	B	infall	χ^2_{SFR}	$\chi^2_{O/H}$
1	1.0	2.00	–	4.0	2.7
2	1.0	3.00	–	0.9	0.7
3	1.0	4.00	–	2.2	2.7
4	1.2	1.00	–	5.4	2.7
5	1.2	1.50	–	1.2	0.7
6	1.2	2.00	–	2.7	1.0
7	1.3	0.80	–	2.0	1.7
8	1.3	1.00	–	1.3	0.8
9	1.3	1.20	–	2.1	0.6
10	1.3	1.50	–	3.3	1.2
11	1.4	0.50	–	3.4	2.0
12	1.4	0.60	–	1.5	1.2
13	1.4	0.70	–	1.6	0.7
14	1.4	0.80	–	2.0	0.6
15	1.4	1.00	–	3.3	0.9
16	2.0	0.04	–	2.5	0.6
17	2.0	0.05	–	1.5	0.6
18	2.0	0.06	–	1.6	0.7
19	2.0	0.10	–	2.1	1.9
20	1.0	2.00	0.001	2.2	3.1
21	1.0	2.00	0.003	2.2	2.5
22	1.0	3.00	0.001	1.2	0.7
23	1.0	3.00	0.003	3.4	0.6
24	1.2	1.00	0.003	1.7	3.1
25	1.2	1.30	0.001	1.2	1.4
26	1.2	1.50	0.001	1.6	0.8
27	1.2	1.50	0.003	3.0	1.4
28	1.4	0.60	0.001	2.0	1.8
29	1.4	0.60	0.003	2.9	3.6
30	1.4	0.70	0.001	1.8	1.0
31	1.4	0.70	0.003	3.2	3.7
32	1.0	3.00	0.003	1.3	2.0
33	1.0	3.20	0.003	1.3	1.3
34	1.0	3.50	0.003	1.8	0.7
35	1.0	4.00	0.003	2.8	1.4
36	1.4	0.60	0.003	3.5	3.2
37	1.4	0.70	0.003	2.3	2.3
38	1.4	0.80	0.003	2.5	1.8
39	2.0	0.05	0.003	2.3	1.6
40	2.0	0.07	0.003	2.0	1.0
41	2.0	0.08	0.003	2.2	0.8
42	1.0	2.00	0.05M	3.3	2.5
43	1.0	3.00	0.05M	1.2	0.6
44	1.4	0.60	0.05M	1.9	1.5
45	1.4	0.70	0.05M	1.8	0.9
46	1.4	0.80	0.05M	2.2	0.7
47	1.4	1.00	0.05M	3.3	0.8

This gas increase enhances our SFR, and the corresponding chemical enrichment is more effective than the infall dilution, thus producing flat or reversed abundance gradients.

4.2 Other spirals

The models of cases (i) and (ii) in better agreement with the Galaxy constraints have been applied also to the spirals M31, M83, M101 and NGC 2403, and their results are compared with the observations in Figs 3 and 4. We have chosen these four galaxies because they are quite different from each other (they range from Sb to Scd in morphological type, from I to III in luminosity class, and from 2.08 kpc to 7.37 kpc in effective radius) and thus provide a good test on the general applicability of our models. The data in the figures are those presented by Díaz & Tosi (1984) and TD85. The solid lines in this case also refer to the best *standard* models computed by TD85.

Despite the fairly small dispersion around the best-fitting line of the overall data for the various spirals in the diagram of Fig. 1, the star formation derived simply from that relation [case (i) models], and providing reasonable predictions for the Milky Way, does not seem to apply also to the other galaxies. In some cases, the SFR is so large that the total gas consumption is achieved significantly earlier than the present epoch. In some other cases, reasonable results can be obtained, but only if we let the proportionality constant, B, of equation (3) vary by two or three orders of magnitude with respect to the value adopted for the Galaxy. Such large variations, in our opinion, have no physical basis, and are therefore incompatible with the hypothesis of general validity of this type of star formation. This failure might be simply due to the fact that the relation between ΣH_2 and log(O/H) given by equation (1) holds only in the present epoch, but it might also be related to different gas and/or metallicity distributions within each single galaxy. The steep distribution in Fig. 1 of the data relative to M31 (diamonds) and to NGC 2403 (open circles) may be interpreted as an indication in this direction. Indeed, it would not be the first time in astrophysics that fairly tight correlations resulting from the combination of several subsamples of galaxies do not turn out to be applicable to individual objects, because the internal distribution in each subsample is significantly different.

In contrast, the bimodal models (e.g. 2 and 28 of Table 2) which work better for one galaxy, work better for the other spirals too, and this may suggest that they are actually more physically meaningful. However, as already found for the Galaxy (Fig. 2b, central panel), all the four bimodal models

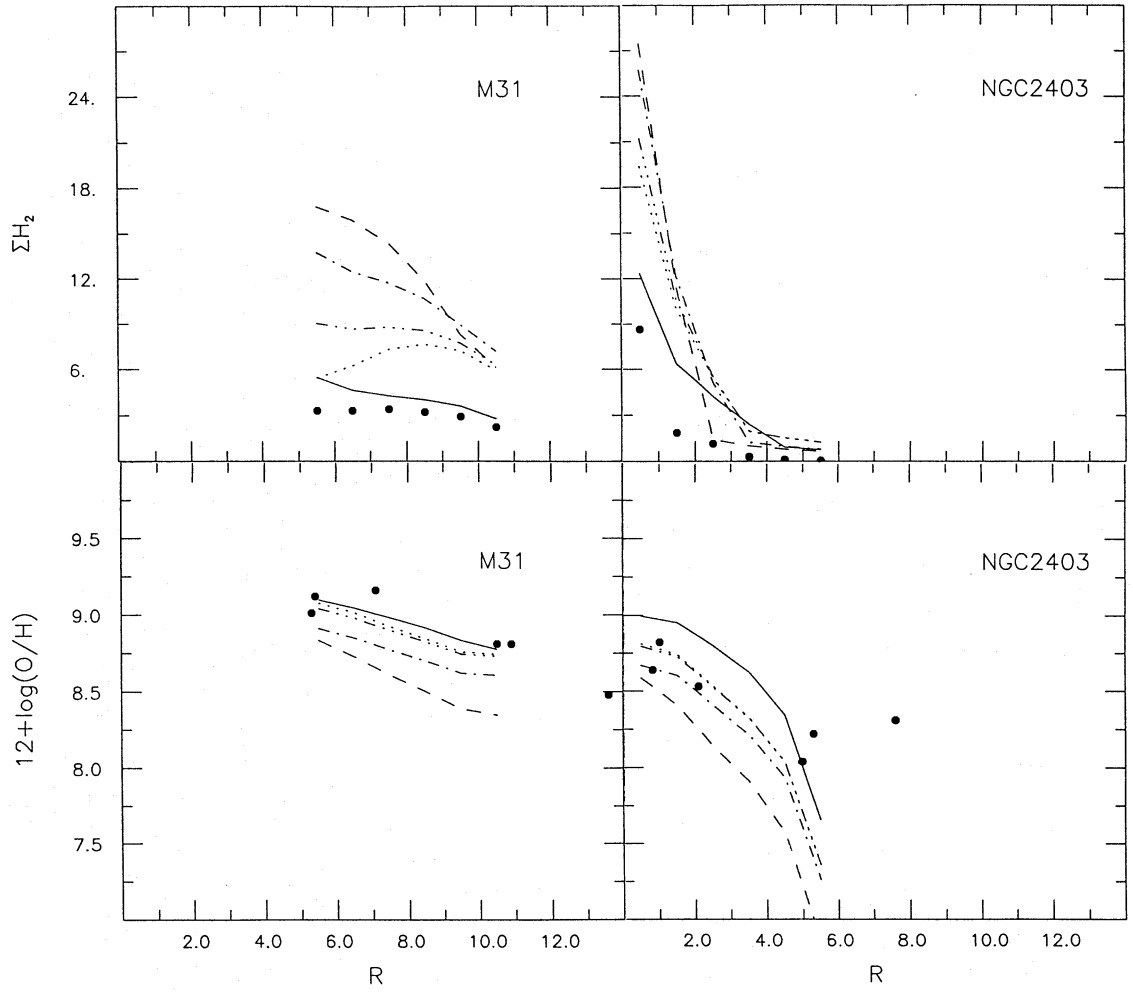

Figure 3. Comparison between observed and predicted radial distributions of the molecular hydrogen density (top) and oxygen abundance (bottom) for M31 and NGC 2403. Symbols are as in Fig. 2(b).

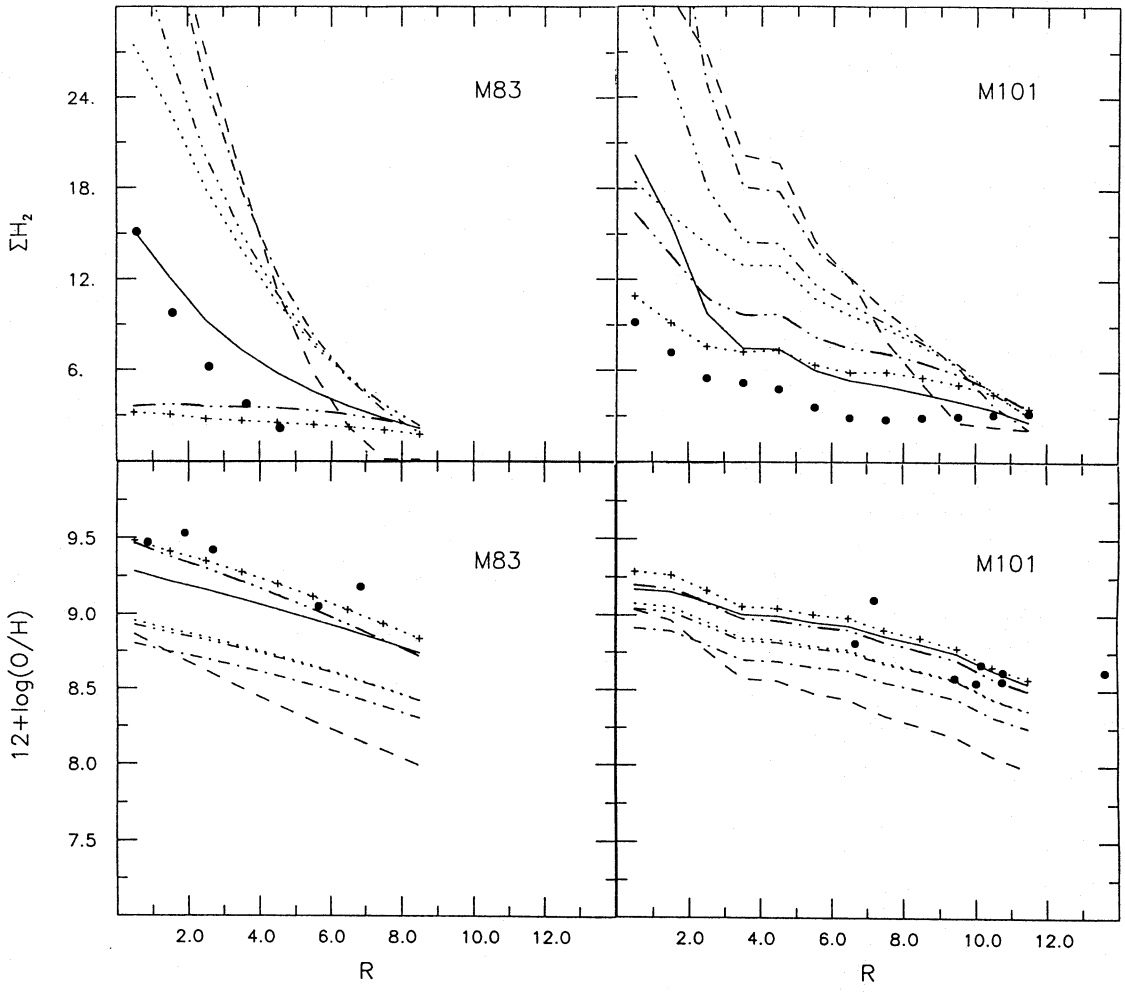

Figure 4. Comparison between observed and predicted radial distributions of the molecular-hydrogen density (top) and oxygen abundance (bottom) for M83 and M101. Symbols are as in Fig. 2(b). The dash-two-dotted and the cross-dotted lines correspond to the additional models referred to in Section 4.2.

predict too much H_2 for the present epoch, generally in the inner galactic regions (top panels of Figs 3 and 4), and all the four bimodal models produce present oxygen abundances which are lower than those derived from *standard* models (bottom panels). In the case of M31 and NGC 2403, this latter result does not affect the comparison with the observational data to a great extent, but for galaxies like M101, and especially M83 (where even the *standard* model underproduces the oxygen abundance), the disagreement becomes significant.

On the other hand, there is no compelling reason for spirals of different morphological type, mass and size to follow exactly the same behaviour as the Milky Way. Small variations of the proportionality constants B and C of the SFR law may be permitted. Indeed, for M101 it is sufficient to increase C by just a factor of 1.5, and for M83 to further increase B by a factor of 2–3 to obtain the predictions for the oxygen abundances represented in Fig. 4 by the dash-two-dotted and cross-dotted lines. Note that with these new models the H_2 distribution in M101 is now better reproduced, but in M83 it is again unsatisfactory (instead of being too steep it is now too flat).

The principal problem with these bimodal models is that the tight correlation between SFR and metallicity does not allow the fine tuning of the various parameters which are necessary to obtain a good agreement with both the observed ΣH_2 and log(O/H). To reduce the overprediction of H_2, we should increase the SFR, but this obviously implies an overproduction of oxygen. The case of M101 shows that we can get close to a good solution, but the case of M83 warns that the process might not converge. This failure warns us that these laws of star formation are perhaps not appropriate for real galaxies.

5 CONCLUSIONS

Following the suggestion by RW88, we have examined in detail the evolution of some spiral galaxies to evaluate if an SFR proportional to the metallicity through the H_2 density can reproduce their observed properties.

We have found that an empirical relation exists between the molecular gas fraction and the logarithm of the oxygen abundance of these nearby spirals. This relation holds in the metallicity range $8 \leq 12 + \log(O/H) \leq 10$ and should not be

extrapolated outside it. Our relation is different from that derived by RW88 from the same set of data.

By computing models of galactic chemical evolution, we have also shown that, contrary to RW88 predictions, an SFR proportional only to ΣH_2 through the metallicity (either linear or logarithmic) does not lead to a solution valid for all the galaxies of our sample. A two-component SFR proportional to both ΣH_2 and Σ_{gas} improves the situation, due to the smooth behaviour provided by the total gas component. Variations (perhaps *ad hoc*) of the proportionality constants from galaxy to galaxy seem necessary, but within a range of values small enough to allow the conclusion that this type of SFR may apply to all the spirals of our sample. We should recall, however, that *standard* models, despite their simpler and perhaps less physical form of SFR, provide results in better agreement with the observational constraints of the various galaxies.

From these arguments it appears that we have not yet reached a satisfactory parametrization for an SFR proportional to the H_2 content. This clearly does not mean that the star formation is not physically related to the molecular gas, but just that it does not allow one to compute detailed and reliable models of galactic chemical evolution with this kind of SFR. Perhaps the best way to overcome this problem would be to avoid any *a priori* parametrization of the SFR and let it derive as a consequence of the complex ambient conditions as in the models by, e.g. Galli & Ferrini (1989). It is important to emphasize, however, that the very good performances of *standard* models where $\psi \propto e^{-t/\tau}$ provide precise information on the time and space behaviour that the resulting SFR should have.

ACKNOWLEDGMENTS

We are indebted to Jan Brand and Gianni Zamorani for their helpful critical suggestions. MT warmly thanks José Zamorano and the Universidad Autónoma for their kind hospitality in Madrid.

REFERENCES

Bhat, C. L., Issa, M. R., Houston, B. P., Mayer, C. J. & Wolfendale, A. W., 1984. In: *Gas in the Interstellar Medium,* p. 39, ed. Gondhalekar, P. M., RAL, UK.

Díaz, A. I. & Tosi, M., 1984. *Mon. Not. R. astr. Soc.,* **208,** 365.

Galli, D. & Ferrini, F., 1989. *Astr. Astrophys.,* **218,** 31.

Lacey, C. G. & Fall, S. M., 1985. *Astrophys. J.,* **290,** 154.

Rana, N. C. & Wilkinson, D. A., 1988. *Mon. Not. R. astr. Soc.,* 497 (RW86).

Rana, N. C. & Wilkinson, D. A., 1988. *Mon. Not. R. astr. Soc.,* **231,** 509 (RW88).

Sanders, D. B., Solomon, P. M. & Scoville, N. Z., 1984. *Astrophys. J.,* **273,** 182.

Shaver, P. A., McGee, R. X., Newton, L. M., Danks, A. C. & Pottasch, S. R., 1983. *Mon. Not. R. astr. Soc.,* **204,** 53.

Talbot, R. J. Jr, 1980. *Astrophys. J.,* **235,** 821.

Tinsley, B. M., 1980. *Fundam. Cosmic Phys.,* **5,** 287.

Tosi, M., 1988. *Astr. Astrophys.,* **197,** 33 (T88).

Tosi, M., 1990. In: *Chemical and Dynamical Evolution of Galaxies,* eds Ferrini, F., Franco, J. & Matteucci, F., in press.

Tosi, M. & Díaz, A. I., 1985. *Mon. Not. R. astr. Soc.,* **217,** 571 (TD85).

Young, J. S. & Scoville, N. Z., 1982. *Astrophys. J.,* **258,** 467.